

# Design of Crawling Motion for a Biped Walking Humanoid with 3-DoF Rigid-flexible Waist

Zelin Huang<sup>1,3</sup>, Xinyang Jiang<sup>1,3</sup>, Huaxin Liu<sup>1,4</sup>, Xuechao Chen<sup>1,3</sup>, Toshio Fukuda<sup>1,2</sup> and Qiang Huang<sup>1,2</sup>

**Abstract**—In order to be applied in complex environment, humanoid robots are desired to have the ability of both biped walking and quadruped crawling. Crawling is a multi-contact motion. If the mechanism is completely rigid, there will be a closed kinematic chain of robot which is likely to cause damage to robot joints. Therefore, the robot needs to have some flexibility in mechanism. However, biped walking requires highly rigid mechanism to maintain walking stability. Consequently, it is a crucial issue to study crawling motion and biped walking motion in case of rigid-flexible mechanism. In this paper, firstly a 3-DoF rigid-flexible waist is proposed. The waist has rigidity when walking and flexibility when crawling. Then a crawling pattern generation algorithm based on CPG is presented, which solves the problem of difficult to plan crawling motion of robot with rigid-flexible mechanism. Finally, the validity of the proposed method is confirmed by experiments.

## I. INTRODUCTION

Humanoid robots are expected to be applied in various circumstances, such as post-disaster relief and post-disaster reconstruction, where usually have complex environment and uneven terrain. Consequently, it is necessary for humanoid robots to have the ability of biped walking and quadruped crawling.

Humanoid robots with crawling ability are relatively difficult to realize stable biped walking. This is mainly because the flexibility of robot is paid more attention than the rigidity of mechanism. iCub [1] imitated infant crawling motion with the help of a CPG network developed by L. Righetti et al. [2]-[6]. Its lower legs were rubbing against the ground when crawling, which hindered its crawling motion. Moreover, its biped walking was slow and not so stable. iStrut [7][8], more precisely a hominid robot, crawled efficiently by extending its rigid connecting elements to single flexible subsystems. But it can not realize biped walking so far.

On the other hand, humanoid robots with good biped walking ability are hard to complete efficient crawling motion. Because crawling is a multi-contact motion and the mechanism of robot is rigid, there will be a closed kinematic chain formed in the robot when crawling. Moreover, unlike

quadruped robots, humanoid robots rarely install force/torque sensors in contact points of crawling motion, such as hands and knees. Once the robot model is inaccurate, the joint damage of robot is likely to be caused and difficult to be reduced by real-time control algorithm. H7 [9] crawled with hands and feet, and there was only one swing limb at a time. The range of its available crawling height was narrow and its crawling speed was slow. HRP-2 [10]-[12] crawled with hands and knees. It yawed its waist to reduce the friction between swing knees and ground. However its waist DoF was not adequate for solving inverse kinematics, its support hands had to slide inward. Furthermore, support hands of H7 and HRP-2 were sliding back and forth when crawling due to the inaccuracy of robot models.

In addition, there are some legged robots have been developed aiming at multi-locomotion recently. Gorilla Robot III [13], a prototype of Multi-Locomotion Robot [14], is able to realize crawling and biped walking. However, its biped walking was relatively slow and not very stable. E2-DR [15] is a torque controlled legged robot capable of biped walking and quadruped crawling, whereas it is larger and heavier than our robot. Thus it has less potential than ours to move in narrower spaces.

In this paper, we aim at developing a humanoid robot with the ability of biped walking and quadruped crawling in case of a rigid-flexible mechanism. We intend to achieve this target from two aspects. Firstly, we propose a 3-DoF rigid-flexible waist, which can maintain rigidity in walking motion and provide flexibility in crawling motion. Secondly, owing to the difficulty of planning crawling motion in case of a rigid-flexible mechanism, we present an algorithm of crawling pattern generation based on CPG which can provide rhythmic control signals to the robot.

The paper is organized as follows: Section II gives the mechanical design of the 3-DoF rigid-flexible waist. The algorithm of crawling pattern generation is described in Section III, which includes the CPG network constructing and the inverse kinematics solving. Section IV shows the results of crawling and walking experiments. Finally, we conclude the study in Section V.

## II. MECHANICAL DESIGN OF WAIST

BHR-6P is a 21-DoF humanoid robot with the height of 1.52m and the weight of 55kg. The kinematics configuration and the specification of BHR-6P are shown in Fig. 1 and Table. 1 respectively. The design concept of BHR-6P is that the robot can be performable for working in various

\*This work was supported in part by the National Natural Science Foundation of China under Grant 91748202, 61320106012, and 61703043.

<sup>1</sup>Intelligent Robotics Institute, School of Mechatronical Engineering, Beijing Institute of Technology, Beijing 100081, China 2120170177@bit.edu.cn

<sup>2</sup>Key Laboratory of Biomimetic Robots of Systems (Beijing Institute of Technology), Ministry of Education, Beijing 100081, China

<sup>3</sup>Internstional Joint Research Laboratory of Biomimetic Robots and Systems (Beijing Institute of Technology), Ministry of Education, Beijing 100081, China

<sup>4</sup>Beijing Innovation Center for Intelligent Robots and Systems, Beijing Institute of Technology, Beijing 100081, China

environment and adaptive to external perturbation. BHR-6P is expected to realize walking, crawling, rolling and recovering from falling down. Waist plays an important role in crawling motion. The agility of waist is helpful in realizing desired stable crawling motion, and the flexibility of waist is efficient in reducing the joint damage caused by the closed kinematic chain.

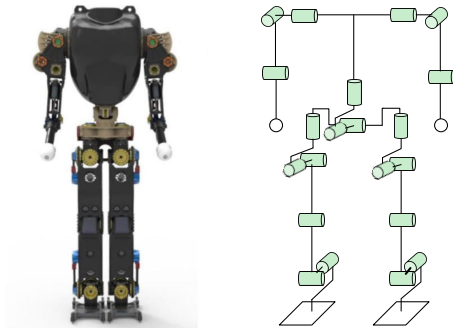


Fig. 1. Left: a picture of BHR-6P. Right: specification of axial composition.

TABLE I  
SPECIFICATION OF BHR-6P

Specification	Value
Height	1.52m
Weight	55kg
Arm	3 DoF (Shoulder: 2 Elbow: 1)
Waist	3 DoF
Leg	6 DoF (Hip: 3 Knee: 1 Ankle: 2)

#### A. The 3-DoF Series-parallel Waist

Fig. 2 shows the mechanical design of 3-DoF series-parallel waist whose prototype has been proposed in our previous work [16]. It utilizes the concept of the human erector spinae. The available movement of waist in three directions is essential in crawling motion since the movement of arms and legs is limited. To reduce the friction between swing knees and ground, the waist needs to yaw to lift swing knees up. To keep contact points motionless, the waist must pitch and roll to realize the desired poses. The pitch and roll rotations are realized by a parallel mechanism while the yaw rotation is achieved by a series joint. The parallel mechanism is a differential mechanism with two linear translation pairs. We use the linear drive unit shown in Fig. 2 to realize the linear translation pair. The waist can achieve pitch movement when the linear translation pairs move in same direction and roll movement when the linear translation pairs move in opposite direction. Meanwhile, the series rotary joint, whose structure is highly integrated, allows a large yaw rotation range.

#### B. Rigid-flexible Device in Linear Drive Unit

Fig. 3 shows the mechanical model of linear drive unit with rigid-flexible device. In this paper, we add this rigid-flexible device to improve the flexibility of our former

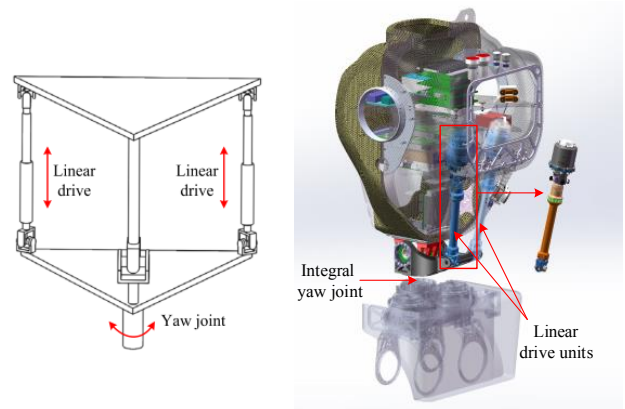


Fig. 2. Left: schematic diagram of the 3-DoF series-parallel waist. Right: 3D mechanical model of the 3-DoF series-parallel waist.

waist. The rigid-flexible device and the linear drive unit are in series connection. The rigid-flexible device consists of ten helical springs, a pair of magnets, a guide belt and a cushion. If the pressure exerted on linear drive unit is less than the maximum attractive force between the magnets, the magnets will stick together and the device will be in rigid state. In rigid state, only linear drive units participate in generating waist pitch angle. If the pressure exerted on linear drive unit is greater than the maximum attractive force, the magnets will separate and the device will be in flexible state. In flexible state, the springs are compressed to provide additional pitch angle of waist according to the pressure. The maximum attractive force which is determined by our empirical knowledge between each pair of magnets is  $200N$ , and the maximum elongation of spring is  $6mm$ .

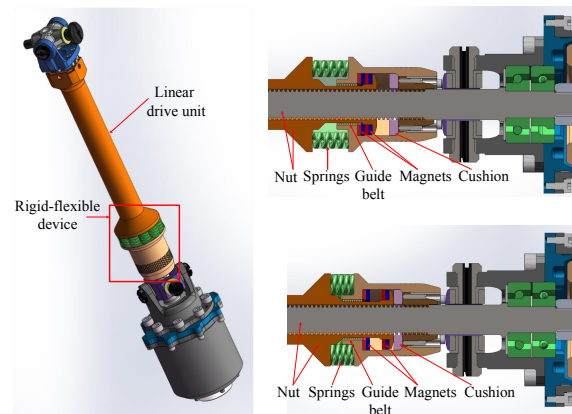


Fig. 3. Left: 3D mechanical model of the linear drive unit with rigid-flexible device. Right top: cutaway view of the rigid-flexible device in rigid state. Right bottom: cutaway view of the rigid-flexible device in flexible state.

#### C. Flexible Rotation in Pitch Direction

Fig. 4 shows the function of rigid-flexible device in crawling motion. In actual robot motion, there is always an

error between actual pose and desired pose because of the inaccurate robot model. If the kinematic chain of robot is closed, the error is more likely to generate extra pressure on robot joints and lead to joint damage. Therefore, we intend to rotate the robot waist compliantly according to the extra pressure to reduce the joint damage. According to our previous crawling experiments, the error in forward direction is larger than the other two directions. Thus it is important for the robot to have flexible rotation in pitch direction since the pitch angles are strongly connected to the forward movement of crawling. When the pressure exerted on waist joint is over the threshold, the magnet pairs in waist will separate and the state of waist will turn to flexible from rigid. Then the springs in two rigid-flexible devices will be compressed and adjust the waist pitch angle compliantly according to the pressure. The maximum adjustable value of pitch angle is  $0.05rad$ , and the stiffness of waist in pitch direction is  $28650N \cdot m/rad$  in flexible state.

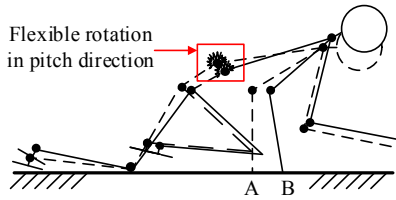


Fig. 4. Schematic diagram of crawling motion of robot with rigid-flexible devices. Suppose the support knee keep motionless when crawling. A is the desired crawling pose, and B is the adjusted crawling pose after the flexible rotation of waist in pitch direction in actual crawling motion

### III. CRAWLING PATTERN GENERATION

Our group have made many contributions on biped walking pattern generation [17]-[21]. Here we present a method of crawling pattern generation for humanoid robots. The method includes two parts. One is generating rhythmic control signals for the body by a CPG network. The other is an analytical approach to solve inverse kinematic of desired crawling motion with the help of 3-DoF waist.

#### A. Design of CPG Network

There are two kinds of CPG models. One is based on neuron models, and the other is based on nonlinear oscillators. The former has a relatively clear biological significance, but it is difficult to perform parameter tuning and dynamics analysis. The latter has the advantages that fewer parameters need to be tuned and more models which are mature are available for reference.

Considering of the convenience of engineering applications, our requirement for the CPG model is to generate stable rhythmic signals for crawling motion and to facilitate programming and parameters tuning. Therefore, we select the modified Hopf oscillator (1)(2)(3) developed by L. Righetti et al. [5][6] as the single control neuron of our CPG network.

This oscillator is stable, has simple tuning of parameters, and is capable of receiving sensory feedback [5].

$$\dot{x} = a(\mu - r^2)x - \omega y \quad (1)$$

$$\dot{y} = b(\mu - r^2)y + \omega x \quad (2)$$

$$\omega = \frac{\omega_{support}}{1 + e^{-\beta y}} + \frac{\omega_{swing}}{1 + e^{\beta y}} \quad (3)$$

where  $r = \sqrt{x^2 + y^2}$ ,  $\sqrt{\mu}$  is the amplitude of the oscillator, and  $\omega$  is the frequency of the oscillator.  $a$ ,  $b$  and  $\beta$  are constants.  $a$  and  $b$  control the convergence speed to the stable limit cycle.  $\beta$  controls the switch speed between support phase and swing phase.

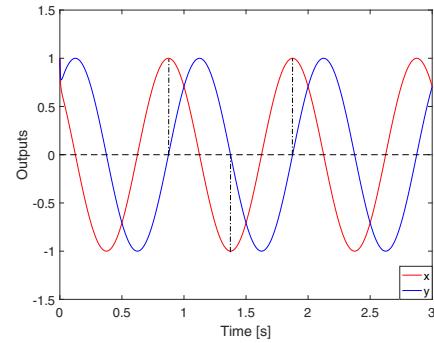


Fig. 5. Output waveforms of the modified Hopf oscillator.

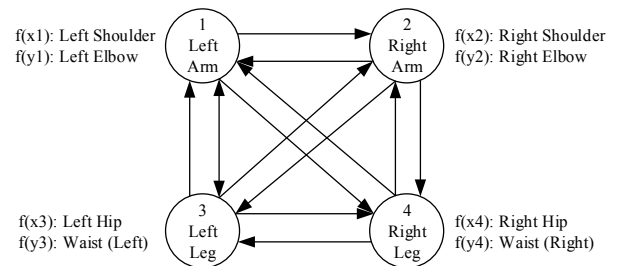


Fig. 6. The modified CPG network. Arm is the forelimb including shoulder, elbow and hand. Leg is the hindlimb including hip, waist and knee here.

According to the output waveforms of the modified Hopf oscillator shown in Fig. 5, the rising phase of  $x$  corresponds to the phase of  $y$  where  $y$  is less than 0 and the falling phase of  $x$  corresponds to the phase of  $y$  where  $y$  is greater than 0. For better motion synchronization between joints in same limb, we modified the original extended CPG network [5] by using one neuron control two joint angles according to this phase relationship between  $x$  and  $y$ . The better motion synchronization can reduce the friction between swing limbs and ground. In our extended CPG network shown in Fig. 6, we use  $x_i$  to control pitch angles of shoulders and hips and use  $y_i$  to control elbow pitch angles and waist yaw angles. The modified CPG network has the same structure as the original one [5]. Therefore, the modified CPG network can

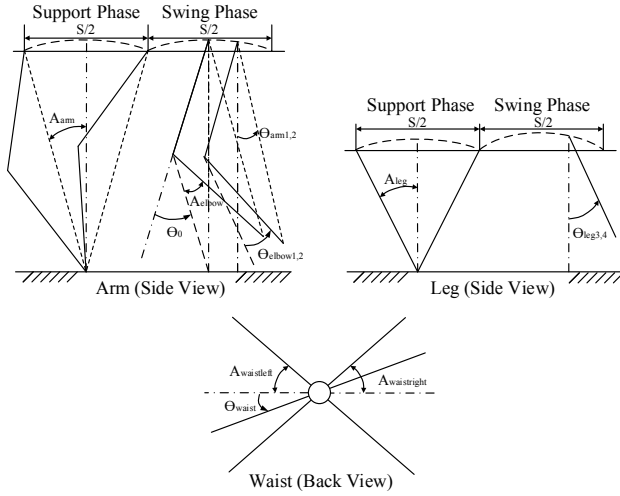


Fig. 7. Definition of related parameters used in this algorithm.  $S$  is the step length.  $\theta_0$  is the elbow pitch angle when the robot in equilibrium position. The equilibrium position is the position that legs (straight lines connecting hips and knees of same limbs) and arms (straight lines connecting shoulders and hands of same limbs) are perpendicular to the ground respectively.  $\theta_x$  ( $x = arm1, 2, leg3, 4, elbow1, 2, waist$ ) is the angle between the current joint position and the equilibrium joint position.  $A_x$  ( $x = arm, leg, elbow, waistright, waistleft$ ) is the amplitude of  $\theta_x$ .

be proved stable [5] by  $H/K$  theorem [22]. It should be noted that we do not apply  $x_i$  and  $y_i$  directly to joint angles, instead we modify them before we apply them. The related parameters used in the following equations are defined in Fig. 7. The equations of the modified CPG network are given as

$$\dot{x}_i = a(\mu_i - r_i^2)x_i - \omega_i y_i \quad (4)$$

$$\dot{y}_i = b(\mu_i - r_i^2)y_i + \omega_i x_i + \sum k_{ij}y_j \quad (5)$$

$$\omega_i = \frac{\omega_{supporti}}{1 + e^{-\beta y_i}} + \frac{\omega_{swingi}}{1 + e^{\beta y_i}} \quad (6)$$

$$\theta_{arm1,2} = x_{1,2} \quad (7)$$

$$\theta_{leg3,4} = x_{3,4} \quad (8)$$

$$\theta_{elbow1,2} = \begin{cases} -\frac{A_{elbow}}{A_{arm}}y_{1,2}, y_{1,2} \leq 0 \\ 0, y_{1,2} > 0 \end{cases} \quad (9)$$

$$\theta_{waist} = \begin{cases} -\frac{A_{waistleft}}{A_{leg}}y_3, y_3 \geq 0, y_4 \leq 0 \\ \frac{A_{waistright}}{A_{leg}}y_4, y_3 > 0, y_4 < 0 \end{cases} \quad (10)$$

where  $r_i = \sqrt{x_i^2 + y_i^2}$ ,  $k_{ij}$  is defined by coupling matrix. In this paper we use the matrix for trot gait [5] which has advantages in both stability and speed.

### B. Analytical Solution to Inverse Kinematics

In this subsection, we provide an analytical solution to inverse kinematics of the desired crawling poses. The desired crawling poses require that support hands and knees should not slide around to improve the crawling efficiency and the torso should not yaw to reduce the possibility of robot

rollover. Thus we make some restrictions given as follows to describe the desired crawling poses.

- The shoulders are supposed to be in same horizontal plane so that the torso will not yaw.
- The shoulders are supposed to be in same coronal plane due to the lack of yaw DoF of arm. Otherwise, support hands would yaw and slide, which would generate unnecessary perturbation.
- The straight lines connecting toes and knees of same limbs should maintain a certain angle to the ground in order to avoid collision between feet and ground.
- The upper legs should remain in sagittal planes to decrease the rotational inertia of lower body when the waist yaws.

The available movement of waist in three directions is necessary in realizing the desired crawling poses. Obtaining the pitch and yaw angles of waist is the key to solving the inverse kinematics of the desired crawling poses. Other angles can be easily calculated according to the waist angles, generated control signals and listed restrictions through analytical way. The analytical method of calculating waist angles is given below.

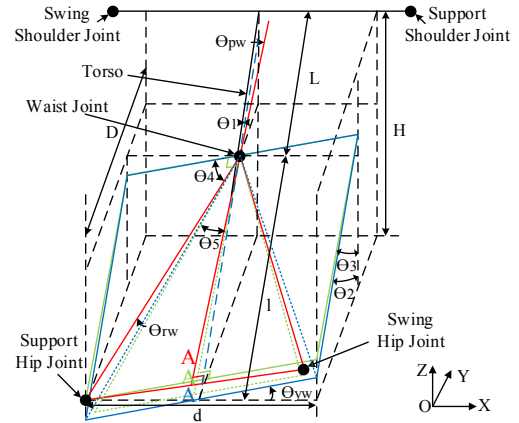


Fig. 8. Definition of parameters used in the inverse kinematics solution and simplified model of crawling robot.  $\theta_{pw}$ ,  $\theta_{rw}$  and  $\theta_{yw}$  are pitch, roll and yaw angles of waist respectively.  $L$  and  $l$  are the length of torso and waist respectively.  $D$  is the distance along  $Y$ -axis between support hip and support shoulder.  $H$  is the distance along  $Z$ -axis between support hip and support shoulder.  $d$  is the straight line distance between two hip joints.  $D$ ,  $H$  and  $\theta_{yw}$  can be easily calculated according to the control signals generated by the CPG network (4)(5)(7)(8). Let plane A be the plane determined by waist joint and two hip joints. The plane with blue boundary is where plane A locates after the yaw motion of waist. The plane with green boundary is where plane A locates after the yaw and pitch motion of waist. The plane with red boundary is where plane A is desired to locate.

Parameters used in the following equations are defined in Fig. 8, and the considered crawling robot model is shown in Fig. 8. Consider the waist in the plane with blue boundary where the waist only yawed. For the law of cosines, the pitch angle of waist is given by

$$\theta_1 = \pi + \arccos \frac{L^2 + l^2 - D^2 - H^2}{2Ll} \quad (11)$$

So that the desired pitch angle of waist in the plane with red boundary is given by

$$\theta_{pw} = \theta_1 - (\theta_2 - \theta_3) \quad (12)$$

$$\theta_2 = \frac{\pi}{2} - \left( \arctan \frac{H}{D} + \arccos \frac{l^2 + D^2 + H^2 - L^2}{2l\sqrt{D^2 + H^2}} \right) \quad (13)$$

$$\theta_3 = \arctan \frac{l \sin \theta_2}{l \cos \theta_2 - 0.5d \sin \theta_2} \quad (14)$$

Consider in the plane with green boundary, the desired roll angle of waist is given by

$$\theta_{rw} = - \left( \frac{\pi}{2} - \theta_4 - \theta_5 \right) \quad (15)$$

$$\theta_4 = \frac{\left( \frac{d}{2 \cos \theta_{yw}} \right)^2 + \left( \frac{d}{2} \right)^2 + l^2 - \left( \frac{l \sin \theta_2}{\sin \theta_3} \right)^2}{\frac{d}{\cos \theta_{yw}} \sqrt{\left( \frac{d}{2} \right)^2 + l^2}} \quad (16)$$

$$\theta_5 = \arctan \frac{0.5d}{l} \quad (17)$$

#### IV. EXPERIMENTS

##### A. Crawling Experiment

Fig. 9 shows the snapshots of crawling experiment on humanoid robot BHR-6P with 3-DoF rigid-flexible waist. The parameters of the CPG network are listed in Table. 2. The crawling speed of BHR-6P reached over  $0.41 \text{ km} \cdot \text{h}^{-1}$ .

TABLE II  
PARAMETERS OF THE CPG NETWORK

Parameter	Value	
	Arm	Leg
$\sqrt{\mu}$	0.327	0.349
$\omega_{support} = \omega_{swing}$	0.121	0.129
a	10050	10050
b	10050	10050
$\beta$	102	102
$A_{arm}$	$18.7^\circ$	-
$A_{leg}$	-	$20^\circ$
$A_{elbow}$	$5^\circ$	-
$A_{waistright} = A_{waistleft}$	-	$15^\circ$

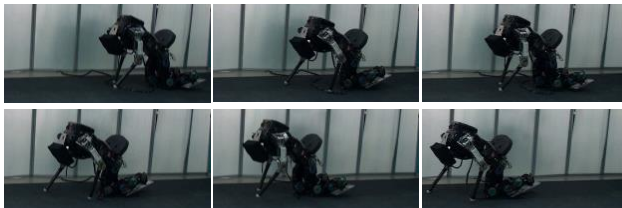


Fig. 9. Snapshots of BHR-6P crawling experiment.

We analyzed the crawling stability by measuring the whole-body dynamics whose limit-cycle behavior can illustrate the whole-body stability [23]. Similar with the quadruped robots, we consider that the pitch dynamics

reflect the up and down movement in pitch plane and the roll dynamics reflect the sinusoid movement of the robot spine [3]. Therefore, the whole-body dynamics of crawling humanoid robots can be obtained by measuring dynamics in pitch and roll planes separately. Fig. 10 shows the dynamics of BHR-6P in pitch and roll planes during experiment, and they are confined to certain limit cycles. Thus BHR-6P with 3-DoF rigid-flexible waist crawled stably in experiment. The quadruped crawling ability of BHR-6P with 3-DoF rigid-flexible waist has been confirmed by crawling experiment.

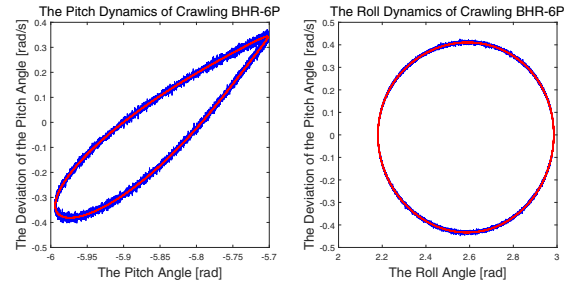


Fig. 10. Right: the pitch dynamics of crawling BHR-6P including the pitch angles of shoulders, hips, knees, elbows, ankles and waist. Left: The roll dynamics of crawling BHR-6P including the roll angles of shoulders, hips, ankles and waist. The red circles indicate the corresponding limited cycles respectively.

##### B. Walking Experiment

Fig. 11 shows the snapshots of walking experiment on humanoid BHR-6P with 3-DoF rigid-flexible waist. The walking speed was over  $1.5 \text{ km} \cdot \text{h}^{-1}$ . The result of walking experiment is shown in Fig. 12. The actual ZMP is within the boundaries of the robot support polygons. Thus the robot walked stably. The biped walking ability of BHR-6P with 3-DoF rigid-flexible waist has been confirmed by walking experiment.



Fig. 11. Snapshots of BHR-6P walking experiment.

#### V. CONCLUSIONS

This paper focused on developing a humanoid robot with the ability of biped walking and quadruped crawling in case of a rigid-flexible mechanism. The contributions of this paper are summarized as follows.

- A 3-DoF rigid-flexible waist was proposed. The waist is rigid in walking motion and flexible in crawling motion.
- An algorithm of crawling pattern generation was presented. The algorithm can provide desired crawling

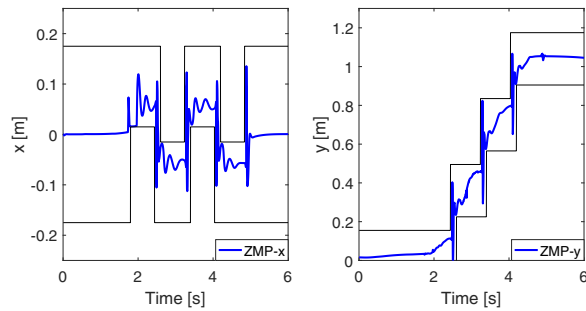


Fig. 12. Actual ZMP in walking experiment of BHR-6P. The black lines indicate the boundaries of the robot support polygons.

pattern for the humanoid robot with the rigid-flexible mechanism and also improve the motion synchronization among robot joints.

- The validity of the proposed method was confirmed by experiments. The humanoid robot with 3-DoF rigid-flexible waist has the ability of stable quadruped crawling and good biped walking.

#### ACKNOWLEDGMENT

The authors would like to give their special thanks to the colleagues in Intelligent Robotics Institute for their patient feedbacks and active discussion.

#### REFERENCES

- [1] G. Metta, G. Sandini, D. Vernon, L. Natale, and F. Nori, The iCub humanoid robot: an open platform for research in embodied cognition, *Proceedings of the 8th workshop on performance metrics for intelligent systems*, pp. 50-56, 2008.
- [2] S. Degallier, L. Righetti, L. Natale, F. Nori, G. Metta, and A. Ijspeert, A modular bio-inspired architecture for movement generation for the infant-like robot iCub, *2nd IEEE RAS & EMBS International Conference on Biomedical Robotics and Biomechanics*, pp. 795-800, 2008.
- [3] L. Righetti, Control of legged locomotion using dynamical systems: design methods and adaptive frequency oscillators, Ph.D. thesis, Dept. Computer Science, EPFL, Lausanne, Switzerland, 2008.
- [4] S. Degallier, L. Righetti, and A. Ijspeert, Hand placement during quadruped locomotion in a humanoid robot: A dynamical system approach, *IEEE-RAS International Conference on Intelligent Robots and Systems*, no. BIOROB-CONF-2009-010, 2007.
- [5] L. Righetti, and A. Ijspeert, Pattern generators with sensory feedback for the control of quadruped locomotion, *IEEE International Conference on Robotics and Automation*, pp. 819-824, 2008.
- [6] L. Righetti, and A. Ijspeert, Design methodologies for central pattern generators: an application to crawling humanoids, *Proceedings of robotics: Science and systems*, no. BIOROB-CONF-2006-004, pp. 191-198, 2006.
- [7] D. Kühn, Design and Development of a Hominid Robot with Local Control in Its Adaptable Feet to Enhance Locomotion Capabilities, Ph.D. thesis, Dept. Informatics and Mathematics, Universität Bremen, Bremen, Germany, 2016.
- [8] D. Kuehn, F. Grimminger, F. Beinertsdorf, F. Bernhard, A. Burchardt, M. Schilling, M. Simnoffske, T. Stark, M. Zenzes, and F. Kirchner, Additional DOFs and sensors for bio-inspired locomotion: Towards active spine, ankle joints, and feet for a quadruped robot, *IEEE International Conference on Robotics and Biomimetics (ROBIO)*, pp. 2780-2786, 2011.
- [9] K. Nishiwaki, J. Kuffner, S. Kagami, M. Inaba, and H. Inoue, The experimental humanoid robot H7: a research platform for autonomous behaviour, *Philosophical Transactions of the Royal Society of London A: Mathematical, Physical and Engineering Sciences*, vol. 365, no. 1850, pp. 79-107, 2007.

- [10] H. Sanada, E. Yoshida, and K. Yokoi, Passing under obstacles with humanoid robots, in *Experimental Robotics*, vol. 45, O. Khatib, V. Kumar, G.J. Pappas, Eds., Berlin, Heidelberg: Springer, 2009, pp. 283-291.
- [11] F. Kabehiro, T. Yoshimi, S. Kajita, M. Morisawa, K. Kaneko, H. Hirukawa, and F. Tomita, Whole body locomotion planning of humanoid robots based on a 3D grid map, *IEEE International Conference on Robotics and Automation*, pp. 1084-1090, 2005.
- [12] F. Kanehiro, H. Hirukawa, K. Kaneko, S. Kajita, K. Fujiwara, K. Harada and K. Yokoi, Locomotion planning of humanoid robots to pass through narrow spaces, *IEEE International Conference on Robotics and Automation*, vol. 1, pp. 604-609, 2004.
- [13] T. Kobayashi, T. Aoyama, M. Sobajima, K. Masafumi, K. Sekiyama, and T. Fukuda, Locomotion selection strategy for multi-locomotion robot based on stability and efficiency, *IEEE/RSJ International Conference on Intelligent Robots and Systems (IROS)*, pp. 2616-2621, 2013.
- [14] T. Fukuda, Y. Hasegawa, K. Sekiyama, and T. Aoyama, *Multilocomotion Robotic Systems: New Concepts of Bio-inspired Robotics*. Springer-Verlag, vol. 81, 2012.
- [15] T. Yoshiike, M. Kuroda, R. Ujino, H. Kaneko, H. Higuchi, S. Iwasaki, Y. Kanemoto, M. Asatani and T. Koshiishi, Development of experimental legged robot for inspection and disaster response in plants, *IEEE/RSJ International Conference on Intelligent Robots and Systems (IROS)*, pp. 4869-4876, 2017.
- [16] W. Zhang, X. Guo, H. Huang, and Q. Huang, Novel design of a 3-DOF series-parallel torso for humanoid robots, *IEEE International Conference on Mechatronics and Automation (ICMA)*, pp. 1149-1154, 2016.
- [17] X. Chen, Z. Yu, W. Zhang, Y. Zheng, H. Huang, and A. Min, Bioinspired Control of Walking With Toe-Off, Heel-Strike, and Disturbance Rejection for a Biped Robot, *IEEE Transactions on Industrial Electronics*, vol. 64, no. 10, pp. 7962-7971, 2017.
- [18] Z. Yu, X. Chen, Q. Huang, W. Zhang, L. Meng, W. Zhang, and J. Gao, Gait planning of omnidirectional walk on inclined ground for biped robots, *IEEE Transactions on Systems, Man, and Cybernetics: Systems*, vol. 46, no. 7, pp. 888-897, 2016.
- [19] X. Chen, Q. Huang, W. Zhang, Z. Yu, J. Li, G. Ma, S. Zhang, and Y. Li, Inverse dynamics control with acceleration optimization on a force-controlled bipedal robot, *IEEE-RAS International Conference on Humanoid Robots (Humanoids)*, pp. 278-283, 2012.
- [20] W. Xu, Q. Huang, J. Li, Z. Yu, X. Chen, and Q. Xu, An improved ZMP trajectory design for the biped robot BHR, *IEEE-RAS International Conference on Humanoid Robots*, pp. 99-104, 2008.
- [21] Q. Huang, Z. Yu, W. Zhang, X. Duan, Y. Huang, and L. Kejie, Generation of humanoid walking pattern based on human walking measurement, *IEEE International Conference on Robotics and Automation (ICRA)*, pp. 569-574, 2011.
- [22] M. Golubitsky, and I. Stewart, Nonlinear dynamics of networks: the groupoid formalism, *Bulletin of the american mathematical society*, vol. 43, no. 3, pp. 305-364, 2006.
- [23] C. Li, R. Lowe, B. Duran, and T. Ziemke, Humanoids that crawl: comparing gait performance of iCub and NAO using a CPG architecture, *IEEE International Conference on Computer Science and Automation Engineering (CSAE)*, vol. 4, pp. 577-582, 2001.